Mathematics

https://www.aimspress.com/journal/Math

AIMS Mathematics, 11(9): 29796–29815.
DOI:10.3934/math.20261182
Received: 26 April 2026
Revised: 30 August 2026
Accepted: 03 September 2026
Published: 15 September 2026

Research article

Equiform kinematics interpreted via dual-space geometry

Ali Abdela Ali, Anas A. M. Arafa and Fahad Abdulaziz Alsidrani*

Department of Mathematics, College of Science, Qassim University, Buraydah, 52571, Saudi Arabia

* **Correspondence:** Email: f.alsedrani@qu.edu.sa.

Abstract: This paper investigates equiform spatial kinematics using dual-vector line geometry. Oriented lines in Euclidean three-space are represented by unit dual vectors or equivalently by normalized Plücker coordinates consisting of a unit direction vector and an orthogonal moment vector. A consistent moving-frame formulation is developed for transformations combining a dual orthogonal motion with a time-dependent uniform scale factor. The condition under which the tangential component of acceleration vanishes is derived while retaining all derivatives of the scale factor. The corresponding line loci are then characterized in Plücker space, with particular attention to Bresse complexes, line congruences, and the associated ruled surfaces. Explicit parametric expressions are obtained for a selected dual spherical motion, and the rigid-body formulation is recovered as the special case of a constant unit scale. The geometric significance of the selected equiform motion is demonstrated through the resulting Bresse complexes, line congruences, and ruled-surface families. Reproducible computational visualizations illustrate the resulting geometric structures. The developed framework provides a line-geometric approach to equiform and rigid-body kinematics with potential applications in mechanism theory, robotics, and computer-aided geometric design.

Keywords: computer simulation; dual-vector calculus; equiform motion; Bresse complex; Plücker coordinates; line congruence; ruled surface; spatial kinematics
Mathematics Subject Classification: 53A17, 53A25, 70B10, 70E15

1. Introduction

A surface is classified as ruled when it is generated by the continuous motion of a straight line in space. Ruled surfaces (RS) constitute some of the fundamental geometric objects in surface theory and geometric modeling, and they play an important role in numerous scientific and engineering applications, including the geometric design and fabrication of mechanical components, spatial kinematics, moving geometry, mathematical physics, and computer-aided geometric design (CAGD). In spatial mechanisms and robotic systems, generating lines may also be interpreted geometrically as axes associated with joints, screws, or line trajectories.

The differential geometry of ruled surfaces has traditionally been developed using vector calculus and classical differential-geometric methods [1]. The study of line trajectories and their differential invariants was subsequently extended through dual vector calculus, providing an effective framework for the geometric analysis of spatial motions [2, 3]. In line geometry, three-dimensional Euclidean space can be investigated through the manifold of its oriented lines, establishing a close connection between ruled-surface geometry, spatial kinematics, and mechanism theory [4, 5].

Dual vector calculus provides a particularly convenient representation of spatial line geometry. In this setting, an oriented line in Euclidean three-space can be represented by a dual unit vector and hence, by a point on the dual unit sphere (DUS). This representation allows the direction and moment of an oriented line to be incorporated within a single dual-geometric object. The classical foundations of this approach are closely related to Study's representation of spatial displacements and line geometry [6]. These ideas were further developed within differential geometry and spatial kinematics, where dual vectors, screws, and related geometric quantities provide compact representations of rotational and translational motion [1, 4].

Within the dual-geometric framework, dual spherical motion (DSM) provides a useful interpretation of spatial motion through curves on the dual unit sphere. The corresponding dual curves determine families of oriented lines and, through the Study correspondence, generate associated ruled surfaces. This connection makes it possible to investigate kinematic quantities and line-geometric invariants simultaneously. In particular, the differential geometry of spatial line trajectories has been studied using dual vector methods, with special attention to their associated ruled surfaces and kinematic invariants [5, 7–9].

Recent developments demonstrate the continuing relevance of dual algebraic and line-geometric techniques in spatial kinematics. Condurache [10] employed dual tensor algebra and dual quaternions in the description of full-body relative spacecraft motion. Wang et al. [11] developed dual-quaternion operations for rigid-body motion and applied them to hand–eye calibration, and Farias et al. [12] provided a comprehensive review of dual-quaternion applications in kinematics, robotics, control, and motion representation. Recent investigations have also continued the geometric study of line congruences and prescribed line trajectories [13, 14]. These contributions illustrate the effectiveness of dual-geometric representations in connecting spatial motion with line geometry and provide further motivation for studying the line structures associated with equiform spatial motions.

Among the geometric objects arising in spatial kinematics, Bresse loci are of particular interest. They are associated with oriented lines whose trajectories satisfy the condition of vanishing tangential acceleration equivalently and the orthogonality of the corresponding velocity and acceleration vectors. In a dual-space formulation, this condition can be investigated through the motion of oriented lines on the dual unit sphere. Although the existing literature provides substantial results on dual spherical motions, line trajectories, ruled surfaces, and dual-quaternion representations, explicit analytical descriptions of Bresse-type loci for equiform spatial motions, together with their associated line-geometric structures, remain comparatively limited.

Motivated by this observation, the present work develops a dual-space formulation for equiform spatial motion and investigates the associated Bresse loci, line congruences, and ruled-surface families. In particular, we consider the dual-space motion

$$\widehat{\mathbf{Y}} = \widehat{\rho}\,\widehat{\mathbf{W}}\,\widehat{\mathbf{y}}, \tag{1.1}$$

where $\widehat{\mathbf{W}}$ is a dual orthogonal transformation, $\widehat{\rho}$ is the dual scale factor, and $\widehat{\mathbf{y}}$ represents an oriented line on the dual unit sphere (DUS), satisfying

$$\widehat{\mathrm{y}}_1^2 + \widehat{\mathrm{y}}_2^2 + \widehat{\mathrm{y}}_3^2 = 1. \tag{1.2}$$

The dual orthogonal rotation matrix is taken in the form

$$\widehat{\mathbf{W}} = \begin{pmatrix} \cos\widehat{\beta}\cos\widehat{\gamma} & \sin\widehat{\beta}\cos\widehat{\gamma} & \sin\widehat{\gamma} \\ -\sin\widehat{\beta} & \cos\widehat{\beta} & 0 \\ -\cos\widehat{\beta}\sin\widehat{\gamma} & \sin\widehat{\beta}\sin\widehat{\gamma} & \cos\widehat{\gamma} \end{pmatrix}. \tag{1.3}$$

Here,

$$\widehat{\beta}(\mathrm{t}) = \beta(\mathrm{t}) + \varepsilon\beta^*(\mathrm{t}), \qquad \widehat{\gamma}(\mathrm{t}) = \gamma(\mathrm{t}) + \varepsilon\gamma^*(\mathrm{t}), \qquad \widehat{\rho}(\mathrm{t}) = \rho(t) + \varepsilon\rho^*(\mathrm{t}) \tag{1.4}$$

are dual-valued functions of the real-time parameter t.

When the real part $\rho(\mathrm{t})$ of the dual scale factor $\widehat{\rho}(\mathrm{t})$ varies with time, the transformation represents a time-dependent equiform motion. The rigid-body case is recovered under the restriction

$$\widehat{\rho}(\mathrm{t}) = 1. \tag{1.5}$$

A constant nonunit dual scale factor, $\widehat{\rho} = \rho + \varepsilon\rho^*$, corresponds to the constant-scale (static) equiform case considered in the subsequent line-geometric analysis.

Within this framework, the Bresse condition is formulated in dual space, and the resulting algebraic constraints are analyzed in terms of the associated line geometry. Particular attention is given to the constant dual-scale case, for which the corresponding Bresse loci and their associated line-geometric structures are derived explicitly. The analytical results are further supported by computer-generated visualizations of the resulting line congruences and ruled surfaces.

1.1. Methodological comparison with modern Lie-group approaches

Whereas classical spatial kinematics traditionally relies on vector calculus and localized dual-spherical configurations, modern theoretical developments heavily utilize geometric mechanics and algebraic group formulations. Specifically, spatial rigid-body displacements are elegantly mapped through Lie-group frameworks, where the special Euclidean group $SE(3)$ captures the structural manifold of rigid motions. In this context, kinematics is treated as an evolution on a Lie manifold, where velocities and accelerations correspond to elements of the associated Lie algebra $\mathfrak{se}(3)$.

To clarify the distinct value of our framework, Table 1 critically contrasts the present dual-space formulation with modern Lie-group methods across key kinematic dimensions.

Table 1. Comparison of Lie-group and dual-space equiform formulations.

Aspect	Lie-group methods	Dual-space equiform formulation
Framework	Rigid motions are represented on $SE(3)$ using Lie-group and Lie-algebra structures.	Oriented lines are represented on the dual unit sphere using dual vectors and the Study correspondence.
Motion model	Rotation and translation are incorporated within the standard rigid-body framework.	The motion is represented by $\widehat{\mathbf{Y}} = \widehat{\rho}\widehat{\mathbf{W}}\widehat{\mathbf{y}}$.
Scaling	Standard $SE(3)$ does not include a time-dependent uniform scaling.	The dual scale factor $\widehat{\rho}(t)$ distinguishes rigid, constant-scale, and time-dependent equiform motions.
Bresse condition	Tangential-acceleration constraints are formulated within the rigid-motion framework.	The condition $\ddot{\widehat{\mathbf{Y}}} \cdot \dot{\widehat{\mathbf{Y}}} = 0$ yields algebraic constraints for the associated Bresse locus.

The comparison in Table 1 highlights the distinct geometric role of the proposed formulation. Unlike standard rigid-motion frameworks, the dual-space approach incorporates the scale factor $\widehat{\rho}(\mathrm{t})$ and enables the Bresse condition to be formulated directly in terms of dual line coordinates.

The main contributions of this paper are as follows:

1) A dual-space formulation of equiform spatial motion is developed, including the corresponding velocity and acceleration conditions.
2) The Bresse locus is characterized through the vanishing tangential acceleration condition.
3) Explicit parametric representations are derived for a selected constant dual-scale motion.
4) The associated line congruences, ruled surfaces, and degenerate configurations are analyzed.
5) Computational visualizations are provided to illustrate the resulting geometric structures.

1.2. Theoretical novelty and differentiation from previous studies

To explicitly demonstrate the theoretical novelty of the present work, it is useful to contrast our formulation with foundational studies in dual-space kinematics. Traditional line-geometric models, including those developed by Köse et al. [2, 3] and Sarıoğlu [15], primarily focused on classical rigid-body spatial motions. In the rigid-body setting, no time-dependent homothetic scaling is introduced, and the scale factor may be represented by $\widehat{\rho}(\mathrm{t}) \equiv 1$. Consequently, the corresponding velocity and acceleration fields are determined by the rotational and translational components of the spatial motion.

In contrast, the present study extends the dual-space formulation to time-dependent equiform spatial motion by introducing the dual scale factor $\widehat{\rho}(\mathrm{t}) = \rho(\mathrm{t}) + \varepsilon\rho^*(\mathrm{t})$, whose components may vary with time. This extension introduces the following three main features:

- **Scale-dependent velocity and acceleration fields:** Unlike the classical rigid-body formulation, the velocity and acceleration expressions explicitly retain the first- and second-order time derivatives of the scale factor, $\dot{\widehat{\rho}}(t)$ and $\ddot{\widehat{\rho}}(t)$. These additional terms describe the coupling between time-dependent homothetic scaling and the rotational part of the spatial motion.
- **Generalization of the Bresse constraint:** The vanishing tangential acceleration condition introduced in Eq (3.1) is formulated for the general equiform motion $\widehat{\mathbf{Y}} = \widehat{\rho}\widehat{\mathbf{W}}\widehat{\mathbf{y}}$. For a time-dependent scale factor, the resulting Bresse condition contains additional terms involving $\dot{\widehat{\rho}}$ and $\ddot{\widehat{\rho}}$. The classical rigid-body condition is recovered as the special case $\widehat{\rho}(t) = 1, \dot{\widehat{\rho}}(t) = 0, \ddot{\widehat{\rho}}(t) = 0$. A constant nonunit dual scale factor similarly yields the constant-scale equiform case considered in the subsequent line-geometric analysis.
- **Scale-dependent line-geometric structures:** The introduction of a time-dependent dual scale factor extends the analysis of Bresse loci, line congruences, and associated ruled surfaces from the rigid-body setting to an equiform framework. Consequently, the resulting line-geometric structures may depend not only on the rotational component of the motion but also on the instantaneous scale and its time derivatives, providing a broader framework for studying the evolution of oriented-line configurations under equiform spatial motions.

Thus, the principal theoretical contribution of the present study is the extension of the classical dual-space kinematic framework from rigid-body motion to time-dependent equiform spatial motion, and the rigid-body and constant-scale equiform motions are recovered as special cases of the general formulation.

Organization of the paper. The remainder of this manuscript is organized as follows.

- **Section 2 (Mathematical preliminaries):** Introduces the fundamental concepts of dual numbers, dual vectors, the dual unit sphere, and the mathematical framework required for the description of spatial line geometry and equiform motion.
- **Section 3 (Kinematic model):** Develops the velocity and acceleration fields associated with the general spatial equiform motion. The resulting kinematic formulation distinguishes among the rigid-body case $\widehat{\rho} \equiv 1$, the constant-scale equiform case $\widehat{\rho}$ = constant $\neq 1$, and the time-dependent equiform case $\widehat{\rho} = \widehat{\rho}(t)$. The mathematical notations and symbols used in the kinematic model are presented in Table 2.
- **Section 4 (Bresse locus and line-complex characterization):** Formulates the Bresse condition in dual space and derives the corresponding algebraic constraints in Plücker coordinates. Particular attention is given to the constant dual-scale case and to the geometric structure and dimensional properties of the resulting Bresse line families.
- **Section 5 (Explicit example and singularity analysis):** Considers a representative dual spherical equiform motion, derives the corresponding explicit algebraic and parametric expressions, and examines the resulting regular, singular, and degenerate configurations.
- **Section 6 (Application):** Presents the computational realization of the derived geometric structures and illustrates the associated Bresse loci, line congruences, and ruled-surface families. The computational procedure, parameter values, and plotting settings are specified to improve the reproducibility of the graphical results.
- **Section 7 (Conclusion and discussion):** Summarizes the principal theoretical and computational findings, discusses the scope and limitations of the proposed dual-geometric formulation, and

outlines possible directions for future research.

Table 2. Summary of mathematical notations and symbols used in the kinematic model.

Symbol	Geometric / Kinematic meaning
t	Real-time parameter of the continuous spatial motion
ε	Dual unit satisfying the algebraic property $\varepsilon^2 = 0$
$\mathbb{D}$	The set of dual numbers $(a + \varepsilon a^*)$
$\mathbb{H}$	Three-dimensional projective line space
$\widehat{\mathbf{U}}, \widehat{\mathbf{V}}$	Fixed and moving orthonormal reference frames on the DUS
$\widehat{\mathbf{W}}(t)$	Dual orthogonal rotation matrix describing frame orientation
$\widehat{\rho}(t)$	Time-dependent uniform dual scaling factor
$\rho(t)$	Real part of the scale factor (governs homothetic deformation)
$\rho^*(t)$	Dual part of the scale factor
$\widehat{\beta}(t), \widehat{\gamma}(t)$	Dual angular parameters controlling directional evolution
$\widehat{\mathbf{Y}}$	Dual line vector representing an oriented spatial line
$\mathbf{y}$	Real direction vector of the spatial line
$\mathbf{y}^*$	Orthogonal moment vector of the spatial line (Plücker moment)
ξ	Real scalar parameter along the straight line locus
ω	Instantaneous angular velocity vector of the moving frame
$\underline{\mathbf{Y}}$	Formulated linear congruence equation in $\mathbb{H}$-space
η, σ	Real parts of the spherical coordinates of the dual unit sphere
η^*, σ^*	Dual parts of the spherical coordinates of the dual unit sphere

2. Mathematical preliminaries

Consider two orthonormal, right-handed frames $\widehat{\mathbf{u}} = (\widehat{\mathbf{u}}_1, \widehat{\mathbf{u}}_2, \widehat{\mathbf{u}}_3)$ and $\widehat{\mathbf{v}} = (\widehat{\mathbf{v}}_1, \widehat{\mathbf{v}}_2, \widehat{\mathbf{v}}_3)$, defined on the dual unit sphere (DUS), each associated with a triple of points on the surface. Each point on the DUS can be uniquely expressed as a linear combination (LCO) of either the u-frame basis vectors $\widehat{\mathbf{u}}_1, \widehat{\mathbf{u}}_2$, and $\widehat{\mathbf{u}}_3$ or the v-frame basis vectors $\widehat{\mathbf{v}}_1, \widehat{\mathbf{v}}_2$, and $\widehat{\mathbf{v}}_3$. Consequently, each point on the DUS admits a unique representation, which defines a corresponding dual vector $\widehat{\mathbf{Y}}$ on the surface:

$$\sum_{i=1}^{3} \widehat{\mathbf{Y}}_i \widehat{\mathbf{u}}_i = \sum_{i=1}^{3} \widehat{\mathbf{y}}_i \widehat{\mathbf{v}}_i. \tag{2.1}$$

Using Eq (2.1), we obtain

$$\widehat{\mathbf{Y}}_i = (\widehat{\mathbf{u}}_1 \cdot \widehat{\mathbf{v}}_1)\widehat{\mathbf{y}}_1 + (\widehat{\mathbf{u}}_2 \cdot \widehat{\mathbf{v}}_2)\widehat{\mathbf{y}}_2 + (\widehat{\mathbf{u}}_3 \cdot \widehat{\mathbf{v}}_3)\widehat{\mathbf{y}}_3. \tag{2.2}$$

Additionally, each vector of the frame field $\widehat{\mathbf{V}}$ can be expressed as a linear combination of the basis vectors $\widehat{\mathbf{u}}_1$, $\widehat{\mathbf{u}}_2$, and $\widehat{\mathbf{u}}_3$, such that

$$\widehat{\mathbf{v}}_k = \sum_{i=1}^{3} \widehat{\alpha}_{ik} \widehat{\mathbf{u}}_i. \tag{2.3}$$

By defining $\widehat{\alpha}_{\mathrm{ik}}\widehat{\mathbf{u}}_{\mathrm{i}} \cdot \widehat{\mathbf{v}}_{\mathrm{k}}$, $\widehat{\mathbf{W}} = (\widehat{\alpha}_{\mathrm{ik}}) = (\alpha_{\mathrm{ik}} + \varepsilon\alpha^{*}_{\mathrm{ik}})$, the transformation between the two frame fields can be written as

$$\widehat{\mathbf{V}} = \widehat{\mathbf{W}}^{\mathrm{T}}\widehat{\mathbf{U}}, \qquad \widehat{\mathbf{Y}} = \widehat{\mathbf{Y}}^{\mathrm{T}}\widehat{\mathbf{U}} = \widehat{\mathbf{y}}^{\mathrm{T}}\widehat{\mathbf{V}}. \tag{2.4}$$

Here, $\widehat{\mathbf{V}} = (\widehat{\mathbf{v}}_1, \widehat{\mathbf{v}}_2, \widehat{\mathbf{v}}_3)^{\mathrm{T}}$, $\widehat{\mathbf{U}} = (\widehat{\mathbf{u}}_1, \widehat{\mathbf{u}}_2, \widehat{\mathbf{u}}_3)^{\mathrm{T}}$, $\widehat{\mathbf{Y}} = (\widehat{\mathbf{Y}}_1, \widehat{\mathbf{Y}}_2, \widehat{\mathbf{Y}}_3)^{\mathrm{T}}$, and $\widehat{\mathbf{y}} = (\widehat{\mathbf{y}}_1, \widehat{\mathbf{y}}_2, \widehat{\mathbf{y}}_3)^{\mathrm{T}} \in \mathbb{D}^3$.

The dual vectors $\widehat{\mathbf{Y}}$ and $\widehat{\mathbf{y}}$ represent the same oriented spatial line with respect to the fixed frame $\widehat{\mathbf{U}}$ and the moving frame $\widehat{\mathbf{V}}$, respectively. Here, $\mathbf{y}$ denotes the unit direction vector of the line, and $\mathbf{y}^*$ denotes its moment vector. To distinguish the line direction from the position of a point on the line, let $\mathrm{x}(\xi)$ denote the position vector of an arbitrary point on the line. Thus,

$$\mathrm{x}(\xi) = \mathrm{x}_0 + \xi y, \qquad \xi \in \mathbb{R}. \tag{2.5}$$

The corresponding moment vector is

$$\mathbf{y}^* = \mathrm{x}_0 \times \mathbf{y}. \tag{2.6}$$

Consequently, the oriented line is represented by the unit dual vector

$$\widehat{\mathbf{y}} = \mathbf{y} + \varepsilon\mathbf{y}^* = \mathbf{y} + \varepsilon(\mathrm{x}_0 \times \mathbf{y}), \tag{2.7}$$

subject to

$$\mathbf{y} \cdot \mathbf{y} = 1, \qquad \mathbf{y} \cdot \mathbf{y}^* = 0. \tag{2.8}$$

The position vectors are related by

$$\widehat{\mathbf{Y}} = \widehat{\rho}\,\widehat{\mathbf{W}}\widehat{\mathbf{y}}, \tag{2.9}$$

where $\widehat{\mathbf{W}}$ is an orthogonal dual matrix describing the orientation of the moving frame $\mathbf{V}$ relative to the fixed frame $\mathbf{U}$. In the adopted kinematic model, the frame field $\mathbf{U}$ is assumed to be stationary, and the vectors $\widehat{\mathbf{u}}_1, \widehat{\mathbf{u}}_2$ of the frame field $\mathbf{V}$ depend on a real parameter t, representing time. Hence, $\mathbf{V}$ undergoes a spatial motion relative to $\mathbf{U}$. Geometrically, this motion can be interpreted as a DSM, in which the DUS K, rigidly attached to the moving frame $\mathbf{V}$, rolls on the DUS K′ attached to the fixed frame $\mathbf{U}$. Accordingly, K′ and K are referred to as the fixed and moving spheres, and the motion is represented by K/K′. When the DUS K′ and K are associated with the line spaces H and H′, respectively, the DSM K/K represents a spatial rigid body motion in three-dimensional space, represented by H/H. Certain points on the moving DUS exhibit remarkable kinematic properties due to their distinctive velocity and acceleration characteristics. The analysis of these characteristic points is addressed in the following section.

Classification of the kinematic scaling factor ρ:

The geometric and kinematic nature of the dual space transformation is fundamentally dictated by the behavior of the dual scaling factor $\widehat{\rho}(\mathrm{t}) = \rho(\mathrm{t}) + \varepsilon\rho^*(\mathrm{t})$. To provide a rigorous mathematical foundation, we explicitly distinguish among three distinct physical cases:

1) **Case 1: $\widehat{\rho}(\mathrm{t}) \equiv 1$ (Pure rigid-body motion):** Under this restriction, the real part $\rho(\mathrm{t})$ remains constantly equal to one, and its time derivatives vanish. The transformation completely recovers classical Euclidean rigid-body motion (H/H′). In this state, distances, angles, and spatial volumes are strictly preserved, and the motion can be geometrically interpreted as the pure rolling of the moving dual unit sphere over the fixed dual unit sphere without any scaling or deformation.

2) **Case 2:** $\widehat{\rho}$(t) = **constant** ≠ 1 **(Static equiform motion):** In this case, the scaling factor possesses a constant value other than unity throughout the motion. Whereas the instantaneous geometric shapes are preserved up to a constant global scale factor, the kinetic velocity and acceleration fields are modified uniformly by a constant multiplier. This represents a static homothetic expansion or contraction superimposed on the rigid-body displacement.
3) **Case 3:** $\widehat{\rho}$(t) = ρ(t) [**or** ρ(t) + $\varepsilon\rho^*$(t)] **(Time-dependent equiform motion):** This represents the general and most comprehensive equiform spatial motion framework investigated in this paper, where the scaling factor varies dynamically as a function of the real-time parameter t. The continuous variation of ρ(t) induces nontrivial, time-dependent homothetic deformations in the Euclidean three-space. Consequently, the resulting velocity and acceleration fields depend explicitly not only on the instantaneous scale ρ(t) but also on its higher-order time derivatives, namely $\dot{\rho}$(t) and $\ddot{\rho}$(t), which directly influence the configuration of the Bresse line complex.

3. Kinematic model

Now, we analyze the points on the moving DUS K for which the tangential component of acceleration vanishes, that is, those satisfying

$$\frac{\mathrm{d}^2\widehat{\mathbf{Y}}}{\mathrm{dt}^2}\cdot\frac{\mathrm{d}\widehat{\mathbf{Y}}}{\mathrm{dt}} = 0, \tag{3.1}$$

which expresses the orthogonality between the dual velocity and the dual acceleration vectors. From (2.9), Eq (3.1) can be written as

$$\frac{\mathrm{d}\widehat{\rho}}{\mathrm{dt}}\frac{\mathrm{d}^2\widehat{\rho}}{\mathrm{dt}^2} + \widehat{\rho}\frac{\mathrm{d}\widehat{\rho}}{\mathrm{dt}}\widehat{\mathbf{y}}^{\mathrm{T}}\frac{\mathrm{d}\widehat{\mathbf{W}}^{\mathrm{T}}}{\mathrm{dt}}\frac{\mathrm{d}\widehat{\mathbf{W}}}{\mathrm{dt}}\widehat{\mathbf{y}} + \widehat{\rho}^2\widehat{\mathbf{y}}^{\mathrm{T}}\frac{\mathrm{d}\widehat{\mathbf{W}}^{\mathrm{T}}}{\mathrm{dt}}\frac{\mathrm{d}^2\widehat{\mathbf{W}}}{\mathrm{dt}^2}\widehat{\mathbf{y}} = 0. \tag{3.2}$$

4. Bresse locus and line-complex characterization

In this section, we investigate the geometric structure of the locus of oriented lines satisfying the vanishing tangential acceleration condition during spatial equiform motion. Let the instantaneous line coordinates in the moving frame be represented by the dual Plücker vector $\widehat{\mathbf{y}} = \mathbf{y} + \varepsilon\mathbf{y}^* \in \mathbb{D}^3$.

The Bresse locus at a fixed instant t is defined as the set of oriented spatial lines satisfying

$$\frac{\mathrm{d}^2\widehat{\mathbf{Y}}}{\mathrm{dt}^2}\cdot\frac{\mathrm{d}\widehat{\mathbf{Y}}}{\mathrm{dt}} = 0. \tag{4.1}$$

For the constant dual-scale case $\widehat{\rho} = \rho+\varepsilon\rho^*, \dot{\widehat{\rho}} = 0$, Eq (3.2) simplifies to $\widehat{\rho}\,\widehat{\mathbf{y}}^{\mathrm{T}}\mathrm{d}\widehat{\mathbf{W}}^{\mathrm{T}}/\mathrm{dt}\ \mathrm{d}^2\widehat{\mathbf{W}}/\mathrm{dt}^2\widehat{\mathbf{y}} = 0$. Substituting $\widehat{\mathbf{W}} = \mathbf{W} + \varepsilon\mathbf{W}^*$ and $\widehat{\mathbf{y}} = \mathbf{y} + \varepsilon\mathbf{y}^*$ and separating the real and dual parts yields

$$\rho\,\mathbf{y}^{\mathrm{T}}\left(\frac{\mathrm{d}\mathbf{W}^{\mathrm{T}}}{\mathrm{dt}}\frac{\mathrm{d}^2\mathbf{W}}{\mathrm{dt}^2}\right)\mathbf{y} = 0, \tag{4.2}$$

and

$$\begin{aligned}&\rho\,\mathbf{y}^{*\mathrm{T}}\left(\frac{\mathrm{d}\mathbf{W}^{\mathrm{T}}}{\mathrm{dt}}\frac{\mathrm{d}^2\mathbf{W}}{\mathrm{dt}^2}\right)\mathbf{y} + \rho\,\mathbf{y}^{\mathrm{T}}\left(\frac{\mathrm{d}\mathbf{W}^{\mathrm{T}}}{\mathrm{dt}}\frac{\mathrm{d}^2\mathbf{W}}{\mathrm{dt}^2}\right)\mathbf{y}^* \\ &+ \rho\,\mathbf{y}^{\mathrm{T}}\left(\frac{\mathrm{d}\mathbf{W}^{\mathrm{T}}}{\mathrm{dt}}\frac{\mathrm{d}^2\mathbf{W}^*}{\mathrm{dt}^2} + \frac{\mathrm{d}\mathbf{W}^{*\mathrm{T}}}{\mathrm{dt}}\frac{\mathrm{d}^2\mathbf{W}}{\mathrm{dt}^2}\right)\mathbf{y} + \rho^*\,\mathbf{y}^{\mathrm{T}}\left(\frac{\mathrm{d}\mathbf{W}^{\mathrm{T}}}{\mathrm{dt}}\frac{\mathrm{d}^2\mathbf{W}}{\mathrm{dt}^2}\right)\mathbf{y} = 0.\end{aligned} \tag{4.3}$$

The direction and moment coordinates also satisfy the Plücker conditions

$$y_1^2 + y_2^2 + y_3^2 = 1 \tag{4.4}$$

and

$$y_1 y_1^* + y_2 y_2^* + y_3 y_3^* = 0. \tag{4.5}$$

Equations (4.2)–(4.5) define the Bresse locus as an algebraic family of oriented lines in Plücker space. In general, the resulting constraints contain quadratic and bilinear terms and therefore do not necessarily define a linear line complex. The dimension and geometric structure of the corresponding line family depend on the independence of these constraints for the particular motion considered. Under special parameter choices, the locus may reduce to lower-dimensional line congruences or degenerate configurations, as illustrated in the following section.

4.1. Regularity conditions and geometric dimensionality

The structural dimension of the resulting Bresse line family depends on the rank and independence of the algebraic constraints formulated in Eqs (4.2)–(4.5) at a given instant t. In general, these relations describe the Bresse complex (BC) within the projective line space $\mathbb{H}$. Under the regularity conditions associated with the considered motion, the corresponding Bresse complex may be represented as a three-parameter family of lines.

At a fixed instantaneous value of the time parameter t, and provided that the corresponding constraints remain independent, the admissible locus may reduce to a two-parameter family of lines. This specialized subfamily constitutes a line congruence in $\mathbb{H}$-space and directly characterizes the geometric trace of the instantaneous spatial motion H/H' induced by the underlying dual spherical equiform motion K/K'.

If the constraint system loses rank for particular parameter values or degenerate kinematic configurations, one or more of the governing relations may become dependent. Consequently, the dimension of the resulting line family may increase, giving rise to higher-dimensional or degenerate configurations. Thus, the precise dimensionality of the Bresse locus is determined by the rank of the corresponding constraint system for the particular motion under consideration.

5. Explicit example and singularity analysis

Next, we examine the DSM $\widehat{\mathbf{Y}} = \widehat{\rho}\,\widehat{\mathbf{W}}\,\widehat{\mathbf{y}}$, where $\widehat{\mathbf{W}}$ is an orthogonal dual transformation matrix [2,16] given by

$$\widehat{\mathbf{W}} = \begin{pmatrix} \cos\widehat{\beta}\,\cos\widehat{\gamma} & \sin\widehat{\beta}\,\cos\widehat{\gamma} & \sin\widehat{\gamma} \\ -\sin\widehat{\beta} & \cos\widehat{\beta} & 0 \\ -\cos\widehat{\beta}\,\sin\widehat{\gamma} & \sin\widehat{\beta}\,\sin\widehat{\gamma} & \cos\widehat{\gamma} \end{pmatrix}. \tag{5.1}$$

Here, $\widehat{\beta}(t) = \beta(t) + \varepsilon\beta^*(t)$, $\widehat{\gamma}(t) = \gamma(t) + \varepsilon\gamma^*(t)$, and $\widehat{\rho}(t) = \rho(t) + \varepsilon\rho^*(t)$ are functions of the real parameter t (time).

For the particular case $\beta(t) = \beta^*(t) = \gamma^*(t) = t, \rho = 2, \rho^* = 1, \gamma = \pi/2$, Eqs (4.2)–(4.5) reduce to

$$y_2 - y_1 y_3 = 0. \tag{5.2}$$

$$-2\left((y_1+2y_2)\sin^2(t)+y_3\cos(t)(1+2\sin(t))\right)y_1^*+\left(4y_3\cos^2(t)-2y_3\sin(t)+(y_1y_2+2y_2)\sin(2t)\right)y_2^*=0. \tag{5.3}$$

$$y_1^2+y_2^2+y_3^2=1. \tag{5.4}$$

$$y_1y_1^*+y_2y_2^*+y_3y_3^*=0. \tag{5.5}$$

The solution of Eqs (5.2)–(5.5) has infinitely many solutions, setting

$$\begin{aligned} y_1 &= p, \qquad |p|< 1,\\ y_2 &= p\sqrt{\frac{1-p^2}{1+p^2}},\\ y_3 &= \sqrt{\frac{1-p^2}{1+p^2}}. \end{aligned} \tag{5.6}$$

Because Eq (5.6) and Eqs (5.2)–(5.5) yield two independent relations in three unknowns, the solution space forms a line congruence.

Let

$$\begin{aligned} y_1^* &= q,\\ y_2^* &= -\frac{2q\left(\left(p+2\sqrt{\frac{1-p^2}{1+p^2}}\right)\sin^2(t)\ \sqrt{\frac{1-p^2}{1+p^2}}\ \cos(t)(1+2\sin(t))\right)}{-4\sqrt{\frac{1-p^2}{1+p^2}}\cos^2(t)+2\sqrt{\frac{1-p^2}{1+p^2}}\sin(t)-\left(p+2\sqrt{\frac{1-p^2}{1+p^2}}\right)\sin(2t)},\\ y_3^* &= q\left(\frac{-p}{\sqrt{\frac{1-p^2}{1+p^2}}}+\frac{2\left(\left(p+2\sqrt{\frac{1-p^2}{1+p^2}}\right)\sin^2(t)\ \sqrt{\frac{1-p^2}{1+p^2}}\ \cos(t)(1+2\sin(t))\right)}{-4\sqrt{\frac{1-p^2}{1+p^2}}\cos^2(t)+2\sqrt{\frac{1-p^2}{1+p^2}}\sin(t)-\left(p+2\sqrt{\frac{1-p^2}{1+p^2}}\right)\sin(2t)}\right), \end{aligned} \tag{5.7}$$

where q is a free parameter. Let $\underline{y}=(y_1,y_2,y_3)$, and $\underline{y}^*=(y_1^*,y_2^*,y_3^*)$. The linear congruence (LC) equation in H is obtained by

$$\underline{L}=\underline{y}\times\underline{y}^*+\xi\,\underline{y}. \tag{5.8}$$

The cross product can be expressed in the form

$$\underline{y}\times\underline{y}^*=\left(y_2y_3^*-y_3y_2^*,\ y_3y_1^*-y_1y_3^*,\ y_1y_2^*-y_2y_1^*\right), \tag{5.9}$$

and from the vector Eq (5.8), we obtain three scalar equations, where

$$\underline{y}\times\underline{y}^{*}=\Bigg(\frac{2\sqrt{\frac{1-p^2}{1+p^2}}\left(\left(p+2\sqrt{\frac{1-p^2}{1+p^2}}\right)\sin^2(t)\ \sqrt{\frac{1-p^2}{1+p^2}}\ \cos(t)\,(1+2\sin(t))\right)}{-4\sqrt{\frac{1-p^2}{1+p^2}}\ \cos^2(t)+2\sqrt{\frac{1-p^2}{1+p^2}}\ \sin(t)-\left(p+2\sqrt{\frac{1-p^2}{1+p^2}}\right)\sin(2t)}$$

$$+\frac{\sqrt{\frac{p^2-p^4}{p^2+p^4}}\,q\left(-p+\frac{2\sqrt{\frac{1-p^2}{1+p^2}}\left(\left(p+2\sqrt{\frac{1-p^2}{1+p^2}}\right)\sin^2(t)\ \sqrt{\frac{1-p^2}{1+p^2}}\ \cos(t)\,(1+2\sin(t))\right)}{-4\sqrt{\frac{1-p^2}{1+p^2}}\cos^2(t)+2\sqrt{\frac{1-p^2}{1+p^2}}\sin(t)-\left(p+2\sqrt{\frac{1-p^2}{1+p^2}}\right)\sin(2t)}\right)}{\sqrt{\frac{1-p^2}{1+p^2}}},$$

$$\frac{q\left(\frac{1-p^2}{1+p^2}-p\left(-p+\frac{2\sqrt{\frac{1-p^2}{1+p^2}}\left(\left(p+2\sqrt{\frac{1-p^2}{1+p^2}}\right)\sin^2(t)\ \sqrt{\frac{1-p^2}{1+p^2}}\ \cos(t)(1+2\sin(t))\right)}{-4\sqrt{\frac{1-p^2}{1+p^2}}\cos^2(t)+2\sqrt{\frac{1-p^2}{1+p^2}}\sin(t)-\left(p+2\sqrt{\frac{1-p^2}{1+p^2}}\right)\sin(2t)}\right)\right)}{\sqrt{\frac{1-p^2}{1+p^2}}}, \tag{5.10}$$

$$q\left(-\sqrt{\frac{1-p^2}{1+p^2}}+\frac{2p\left(\left(p+2\sqrt{\frac{1-p^2}{1+p^2}}\right)\sin^2(t)+\sqrt{\frac{1-p^2}{1+p^2}}\ \cos(t)(1+2\sin(t))\right)}{4\sqrt{\frac{1-p^2}{1+p^2}}\ \cos^2(t)-2\sqrt{\frac{1-p^2}{1+p^2}}\ \sin(t)+\left(p+2\sqrt{\frac{1-p^2}{1+p^2}}\right)\sin(2t)}\right)\Bigg).$$

$$\underline{y}=\left(p,p\sqrt{\frac{1-p^2}{1+p^2}},\sqrt{\frac{1-p^2}{1+p^2}}\right),\quad |p|<1. \tag{5.11}$$

The configuration space of the equiform motion is determined through the family of line congruences (LC) $\underline{L}(p,q,\xi,t)$, which characterizes the Bresse complex associated with the considered dual spherical motion.

The functions $\widehat{\beta}(t),\widehat{\gamma}(t)$, and $\widehat{\rho}(t)$ are selected to provide an analytically tractable representative case of dual spherical equiform motion. Here, $\widehat{\beta}(t)$ and $\widehat{\gamma}(t)$ determine the angular evolution of the dual spherical direction and therefore control its rotational geometric behavior, whereas $\widehat{\rho}(t)$ represents the time-dependent uniform scale factor and accounts for the equiform component of the motion. This parameterization is chosen to obtain explicit expressions for the Bresse condition and the associated line families while retaining nontrivial rotational and scaling effects. The resulting general kinematic formulation and Bresse condition do not depend on this particular parameterization.

However, the explicit closed-form expressions for the Bresse complex, line congruences, and ruled surfaces derived in the subsequent analysis are specific to the selected functions $\widehat{\beta}(\mathrm{t}), \widehat{\gamma}(\mathrm{t})$, and $\widehat{\rho}(\mathrm{t})$. Thus, the selected case should be regarded as a representative analytical example rather than a general characterization of all dual spherical equiform motions. Accordingly, conclusions concerning the explicit parameterizations and geometric configurations obtained in this section are restricted to the selected parameterization, whereas the underlying dual-space kinematic formulation and Bresse condition are applicable more generally.

5.1. Geometric interpretation of the line structures

Figures 1–3 illustrate representative geometric configurations of the Bresse line family obtained by fixing selected parameters. Figure 1 shows how fixing p produces reduced families of lines, while Figure 2 illustrates the variation of the corresponding spatial configurations with ξ. Figure 3 presents further parameter slices, showing how the Bresse family generates lower-dimensional line congruences. These visualizations complement the analytical results and provide a geometric interpretation of the associated line structures and their variations under the selected parameter values.

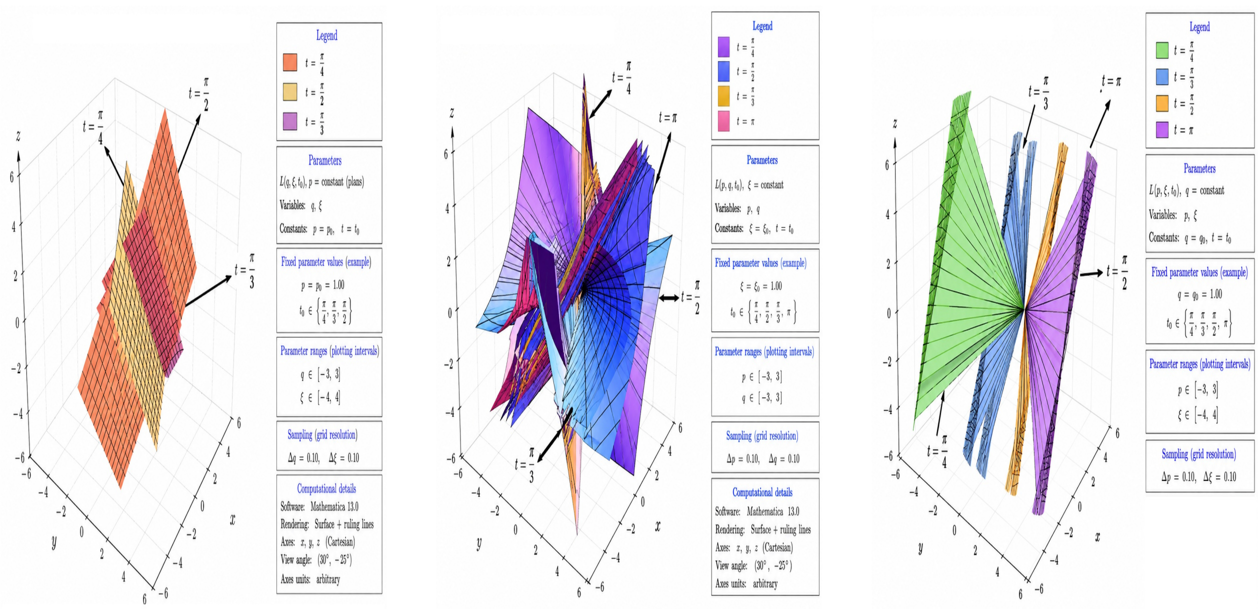

(a) $\underline{\mathrm{L}}(q, \xi, \mathrm{t}^0)$, p = constant (plans). **(b)** $\underline{\mathrm{L}}(\mathrm{p}, \mathrm{q}, \mathrm{t}^0)$, ξ = constant. **(c)** $\underline{\mathrm{L}}(\mathrm{p}, \xi, \mathrm{t}^0)$, q = constant.

Figure 1. t-Family of degenerate (RS) $\underline{\mathrm{L}}(\mathrm{p}, \mathrm{q}, \xi, \mathrm{t})$.

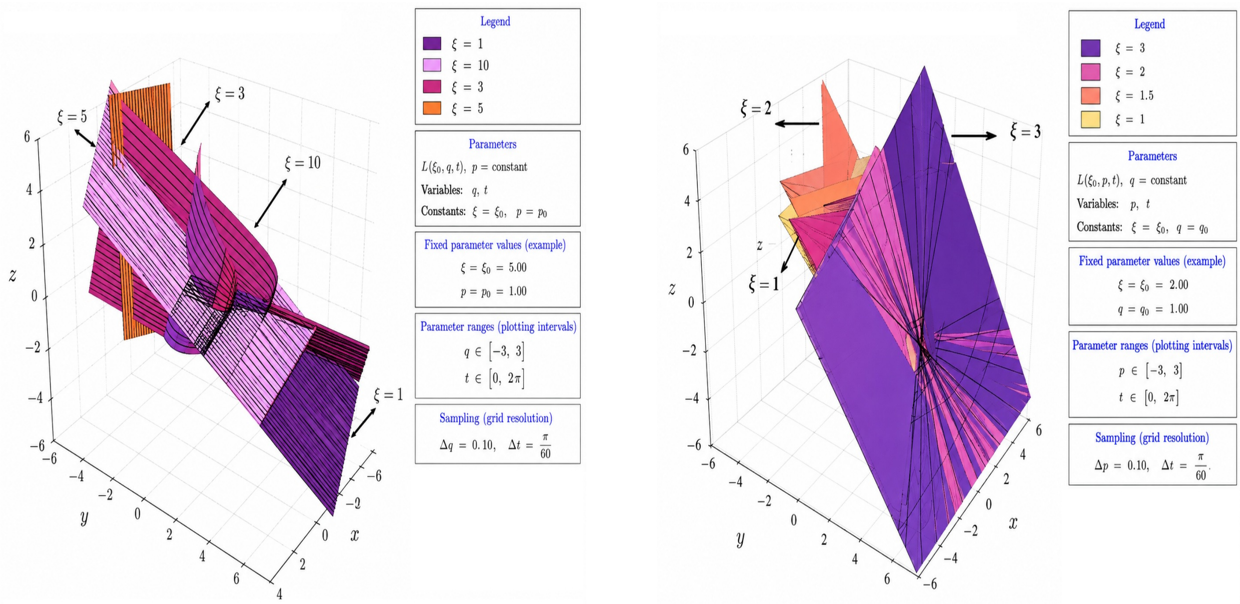

(a) $\underline{L}(\xi^0, q, t)$, p = constant. **(b)** $\underline{L}(\xi^0, p, t)$, q = constant.

Figure 2. ξ-Family of degenerate (RS) $\underline{L}(p, q, \xi, t)$.

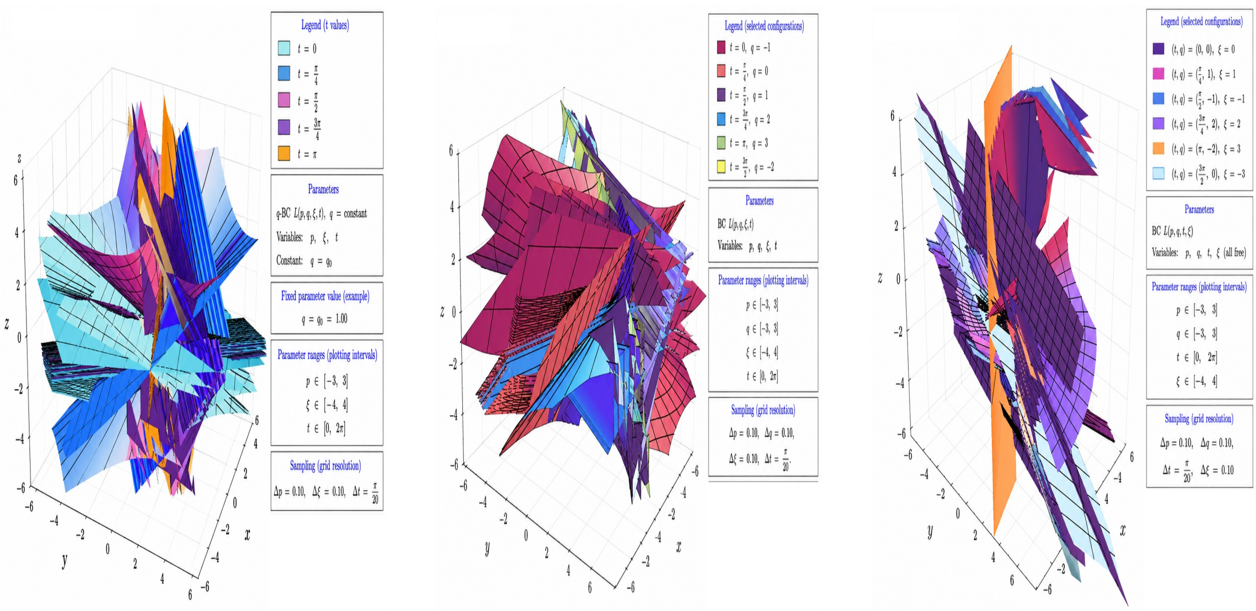

(a) q-BC $\underline{L}(p, q, \xi, t)$, q = constant. **(b)** BC $\underline{L}(p, q, \xi, t)$. **(c)** BC $\underline{L}(p, q, t, \xi)$.

Figure 3. BC of family line congruences (LC).

5.2. *The spherical motion of the equiform motion*

The point $\widehat{y}$ on K is mapped to $\widehat{\mathbf{Y}} = \widehat{\rho}\,\widehat{\mathbf{W}}\,\widehat{\mathbf{y}}$:

$$\begin{aligned}\widehat{\mathbf{Y}}(\mathrm{p},\mathrm{q},\mathrm{t}) &= \mathrm{t}^2\,\mathbf{W}\,\mathbf{y} + \varepsilon\left((\mathbf{W} + \mathrm{t}^2\mathbf{W}^*)\mathbf{y} + \mathrm{t}^2\,\mathbf{W}\,\mathbf{y}^*\right)\\ &= \mathbf{Y} + \varepsilon\mathbf{Y}^*.\end{aligned} \tag{5.12}$$

Thus, we derive the LC equation in $\mathbb{H}$ as follows:

$$\underline{\mathbf{Y}}(\mathrm{p},\mathrm{q},\mathrm{t},\xi) = \mathbf{Y}\times\mathbf{Y}^* + \xi\,\mathbf{Y}, \tag{5.13}$$

where

$$\begin{aligned}\mathbf{Y} &= \left(\mathrm{y}_3\,\mathrm{t}, \mathrm{y}_2\,\mathrm{t}\cos(\mathrm{t}) - \mathrm{x}_1\,\mathrm{t}\sin(\mathrm{t}), -\mathrm{y}_2\,\mathrm{t}\sin(\mathrm{t}) - \mathrm{y}_1\,\mathrm{t}\cos(\mathrm{t})\right),\\ \mathbf{Y}^* &= (-\mathrm{y}_1\,\mathrm{t}^2\cos(\mathrm{t}) - \mathrm{y}_2\,\mathrm{t}^2\sin(\mathrm{t}) + \mathrm{y}_3 + \mathrm{y}_3^*\,\mathrm{t},\\ &\quad -\mathrm{y}_1\,\mathrm{t}^2\cos(\mathrm{t}) + \mathrm{y}_1\sin(\mathrm{t}) + \mathrm{y}_2\cos(\mathrm{t}) - \mathrm{y}_2\,\mathrm{t}^2\sin(\mathrm{t}) + \mathrm{y}_2^*\,\mathrm{t}\cos(\mathrm{t}) - \mathrm{y}_1^*\,\mathrm{t}\sin(\mathrm{t}),\\ &\quad -\mathrm{y}_1\cos(\mathrm{t}) + \mathrm{y}_1\,\mathrm{t}^2 - \mathrm{y}_2\mathrm{t}^2\cos(\mathrm{t}) - \mathrm{y}_2\sin(\mathrm{t}) - \mathrm{y}_3\,\mathrm{t}^2 - \mathrm{y}_2^*\,\mathrm{t}\sin(\mathrm{t}) - \mathrm{t}\,\mathrm{y}_2^*\,\mathrm{t}\sin(\mathrm{t}) - \mathrm{t}\,\mathrm{y}_1^*\cos(\mathrm{t})).\end{aligned} \tag{5.14}$$

From the vectors $\mathbf{y}$ and $\mathbf{y}^*$, it is easy to display the family of LC $\mathbf{Y}(\mathrm{p},\mathrm{q},\mathrm{t},\xi)$ as shown in the figures. The one-parametric family of ruled surfaces in Figure 4 is a degenerate family of developable ruled surfaces (intersection planes). The one-parametric family of ruled surfaces in Figure 5 is a degenerate family of parallel planes. From Figures 6(a)–7(b), we obtain the 4-parametric family of lines. The corresponding line space, consisting of ruled surfaces, line congruences, and line complexes, is illustrated in Figure 7(c).

5.3. *Geometric insights from Figures 4 and 5*

Figures 4 and 5 illustrate representative line and ruled-surface configurations obtained for the selected constant dual scale $\widehat{\rho} = 2 + \varepsilon$. Figure 4 shows how fixing selected parameters produces reduced ruled-surface families, whereas Figure 5 illustrates the corresponding planar and spatial line configurations for different parameter choices. These visualizations complement the analytical results by showing how the Bresse line family generates distinct geometric structures under the prescribed kinematic constraints.

5.4. *Geometric insights from Figures 6 and 7*

Figures 6 and 7 illustrate representative parameter slices of the four-dimensional line space through its associated ruled-surface representations in Euclidean three-space. By fixing selected combinations of the dual parameters $(\eta, \eta^*, \sigma, \sigma^*)$, lower-dimensional families of lines are obtained and visualized. The figures show how variations in these parameters modify the spatial arrangement and geometric form of the corresponding ruled structures, thereby providing a visual interpretation of the line-space parameterization and its associated geometric configurations.

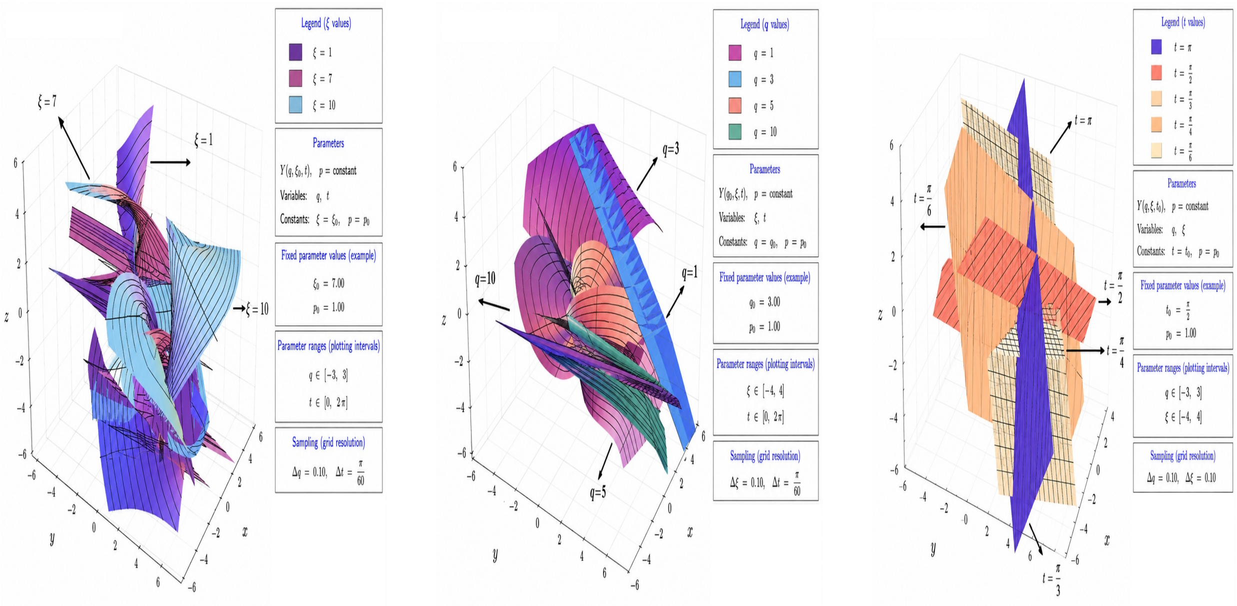

(a) $\mathbf{Y}(q, \xi^0, t)$, $\quad p = \text{constant}$. **(b)** $\mathbf{Y}(q^0, \xi, t)$, $\quad p = \text{constant}$. **(c)** $\mathbf{Y}(q, \xi, t^0)$, $\quad p = \text{constant}$.

Figure 4. 1-Parametric family of (RS) $\underline{\mathbf{y}}(p, q, \xi, t)$.

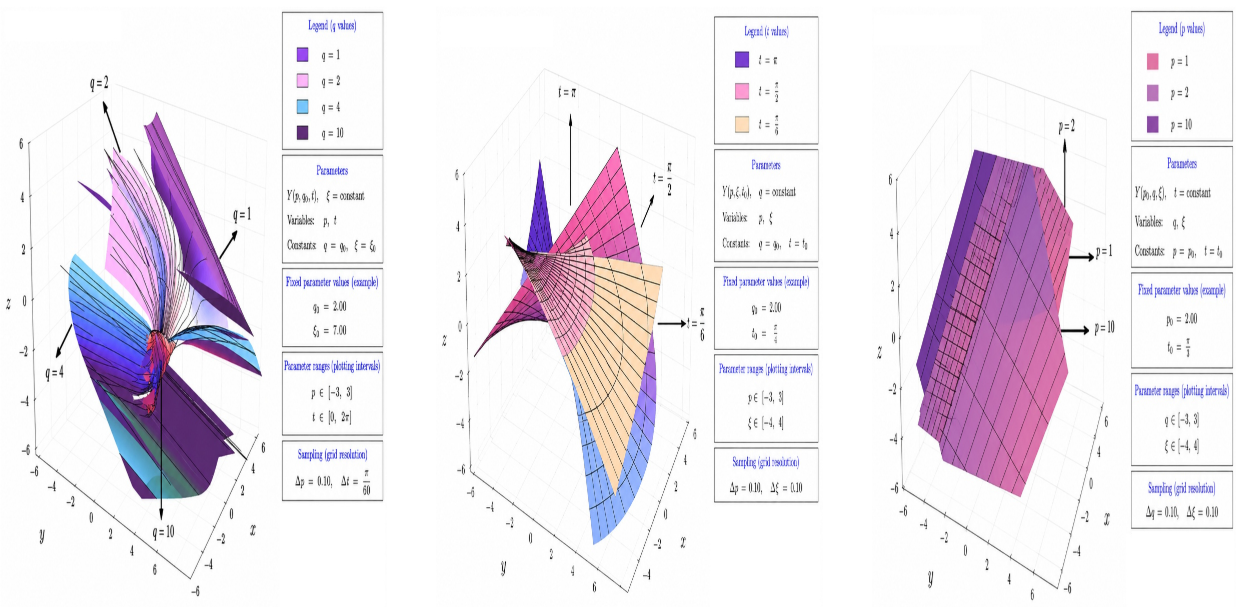

(a) $\mathbf{Y}(p, q^0, t)$, $\quad \xi = \text{constant}$. **(b)** $\mathbf{Y}(p, \xi, t^0)$, $\quad q = \text{constant}$. **(c)** $\mathbf{Y}(p^0, q, \xi)$, $\quad t = \text{constant}$.

Figure 5. 1-Parametric family of (RS) $\underline{\mathbf{y}}(p, q, \xi, t)$.

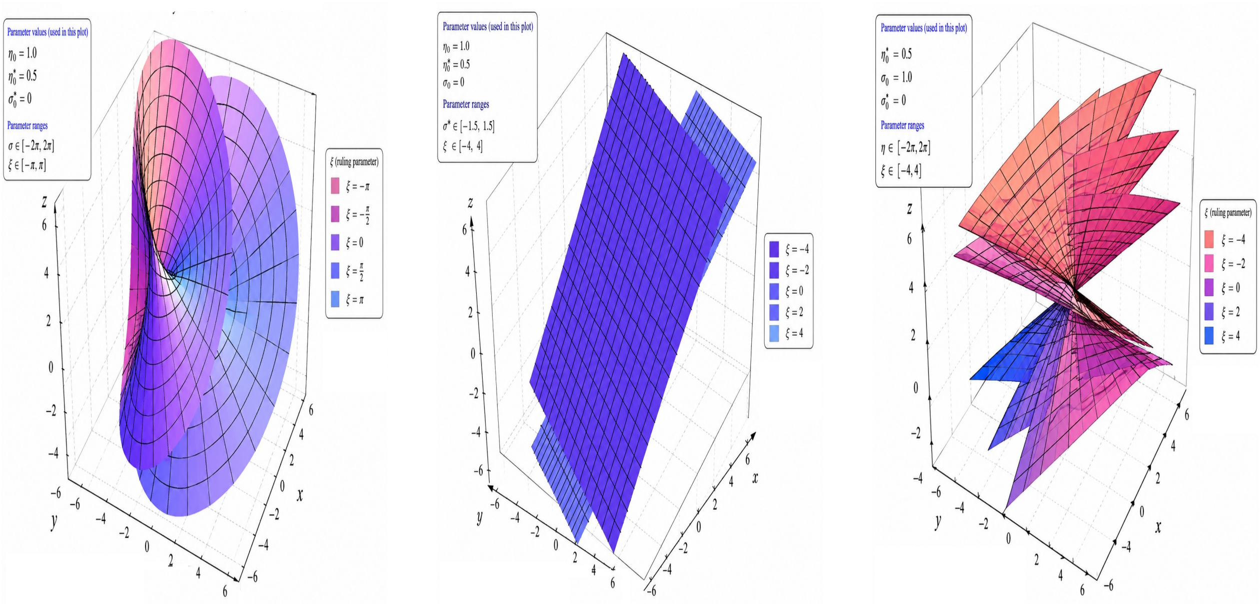

(a) RS $\underline{\mathbf{y}}(\eta^0, \eta^{*0}, \sigma, \sigma^{*0}, \xi) = \underline{\mathbf{y}}(\sigma, \xi)$. **(b)** RS $\underline{\mathbf{y}}(\eta^0, \eta^{*0}, \sigma^0, \sigma^*, \xi) = \underline{\mathbf{y}}(\sigma^*, \xi)$. **(c)** RS $\underline{\mathbf{y}}(\eta, \eta^{*0}, \sigma^0, \sigma^{*0}, \xi) = \underline{\mathbf{y}}(\eta, \xi)$.

Figure 6. 4-Parametric family of lines (line space).

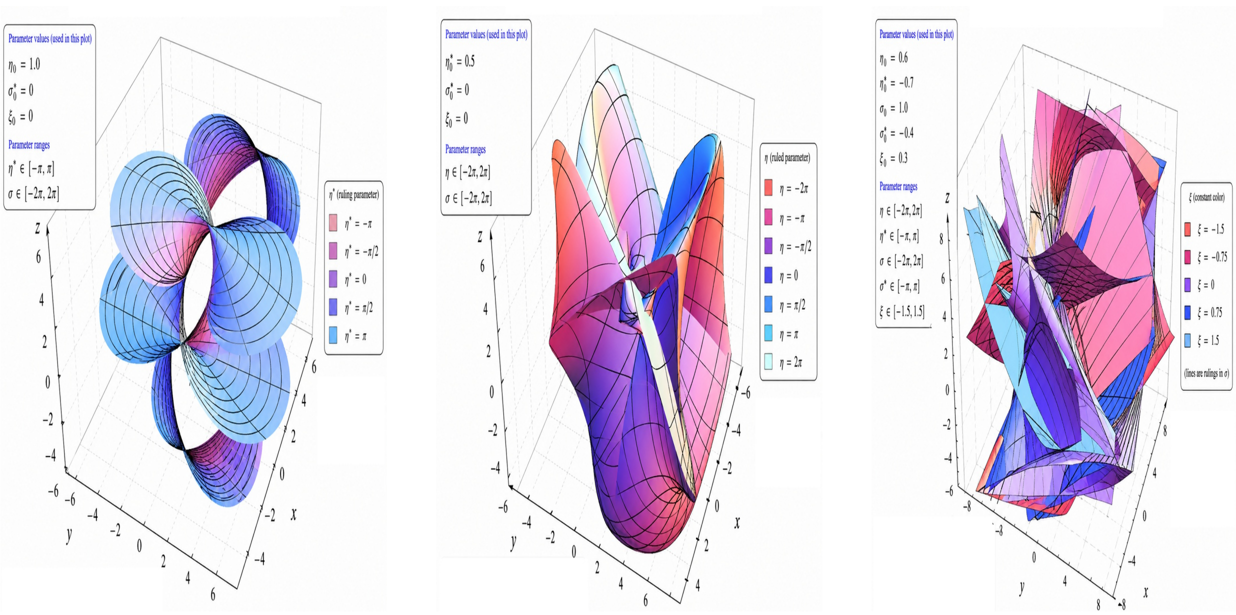

(a) RS $\underline{\mathbf{y}}(\eta^0, \eta^*, \sigma, \sigma^{*0}, \xi^0) = \underline{\mathbf{y}}(\eta^*, \sigma)$. **(b)** RS $\underline{\mathbf{y}}(\eta, \eta^{*0}, \sigma, \sigma^{*0}, \xi^0) = \underline{\mathbf{y}}(\eta, \sigma)$. **(c)** RS $\underline{\mathbf{y}}(\eta, \eta^*, \sigma, \sigma^*, \xi)$.

Figure 7. 4-Parametric family of lines (line space).

6. Application

In the line space, the dual unit sphere $\widehat{y}_1^2 + \widehat{y}_2^2 + \widehat{y}_3^2 = 1$ is not represented. Ultimately, we generate its graph using computer assistance. The equation in parametric form of the dual unit sphere can be expressed in the form

$$\widehat{\mathrm{y}}_1 = \sin\widehat{\eta}\sin\widehat{\sigma}, \qquad \widehat{\mathrm{y}}_2 = \sin\widehat{\eta}\cos\widehat{\sigma}, \qquad \widehat{\mathrm{y}}_3 = \cos\widehat{\eta}, \tag{6.1}$$

where $\widehat{\eta} = \eta + \varepsilon\eta^*$, and $\widehat{\sigma} = \sigma + \varepsilon\sigma^*$.

Separating the real and dual parts of Eq (6.1) gives

$$\mathrm{y}_1 = \sin\eta\sin\sigma, \qquad \mathrm{y}_2 = \sin\eta\cos\sigma, \qquad \mathrm{y}_3 = \cos\eta, \tag{6.2}$$

and

$$\begin{aligned} \mathrm{y}_1^* &= \eta^*\cos\eta\sin\sigma + \sigma^*\sin\eta\cos\sigma, \\ \mathrm{y}_2^* &= \eta^*\cos\eta\cos\sigma - \sigma^*\sin\eta\sin\sigma, \\ \mathrm{y}_3^* &= -\eta^*\sin\eta. \end{aligned} \tag{6.3}$$

These expressions satisfy the Plücker conditions in Eq (2.8), and the corresponding oriented line in Euclidean three-space is parameterized by

$$\mathbf{x}(\eta,\eta^*,\sigma,\sigma^*,\xi) = \mathbf{y}\times\mathbf{y}^* + \xi\mathbf{y}, \qquad \xi\in\mathbb{R}. \tag{6.4}$$

Using Eqs (6.2) and (6.3), we obtain

$$\begin{aligned} \mathbf{y}\times\mathbf{y}^* = (&-\eta^*\cos\sigma + \sigma^*\sin\eta\cos\eta\sin\sigma, \\ &\eta^*\sin\sigma + \sigma^*\sin\eta\cos\eta\cos\sigma, \\ &-\sigma^*\sin^2\eta). \end{aligned} \tag{6.5}$$

Hence, the line-space representation becomes

$$\begin{aligned} \mathbf{x}(\eta,\eta^*,\sigma,\sigma^*,\xi) = (&-\eta^*\cos\sigma + \sigma^*\sin\eta\cos\eta\sin\sigma + \xi\sin\eta\sin\sigma, \\ &\eta^*\sin\sigma + \sigma^*\sin\eta\cos\eta\cos\sigma + \xi\sin\eta\cos\sigma, \\ &-\sigma^*\sin^2\eta + \xi\cos\eta). \end{aligned} \tag{6.6}$$

The four independent parameters η, η^*, σ, and σ^* determine the corresponding family of oriented lines, and ξ parameterizes the points along each individual line. By fixing selected combinations of these parameters, lower-dimensional line families and their associated ruled surfaces are obtained. These parameter reductions provide the geometric configurations illustrated in the following figures.

6.1. Computational implementation and reproducibility

All geometric visualizations, line congruences, and ruled surfaces presented in this study were generated using Wolfram Mathematica (v13.0). The computational procedure was implemented as follows:

1) **Symbolic computation:** Dual-number operations ($\varepsilon^2 = 0$) and the corresponding dual-vector relations were evaluated symbolically using the derived parametric equations.
2) **Numerical sampling:** The parameter $\xi \in [-10, 10]$ was sampled with $\Delta\xi = 0.1$, and $\mathrm{t} \in [0, \pi]$ was sampled with $\Delta\mathrm{t} = \pi/60$. The free parameters p and q were sampled over their prescribed domains using a uniform step of 0.05.
3) **Visualization:** The resulting parametric line and ruled-surface representations were visualized using `ParametricPlot3D`. Parameter values and ranges used for individual plots are specified in the corresponding figure captions.

6.2. *Potential applications to robotic kinematics*

The dual-space formulation developed in this study provides a line-geometric framework that may be useful in the kinematic analysis of spatial mechanisms and robotic systems. In such applications, joint axes and other oriented lines can be represented by dual unit vectors, allowing their geometric evolution to be studied within the same dual-space setting.

In particular, the Bresse condition identifies line configurations for which the tangential component of acceleration vanishes at a given instant. This property may provide a geometric criterion for studying special instantaneous configurations of spatial mechanisms. Moreover, the line congruences and ruled-surface families obtained from the proposed formulation offer geometric representations that may be useful for visualizing the evolution of families of joint axes or line trajectories.

The present study is theoretical and does not consider a specific robot architecture, manipulator Jacobian, actuator dynamics, or experimental motion data. Therefore, direct conclusions regarding robotic singularities, energy consumption, or control performance are beyond the scope of the present work. Future studies may investigate these applications by integrating the proposed dual-space formulation with specific robotic mechanisms and numerical or experimental validation.

7. Conclusions and discussions

This study developed a dual-space framework for the geometric analysis of equiform spatial motion and its associated line structures. Oriented lines were represented on the dual unit sphere, allowing the rotational, translational, and scaling components of the motion to be incorporated within a unified dual-vector formulation. The velocity and acceleration relations were derived for a general time-dependent dual scale factor $\widehat{\rho}(t)$, with rigid and constant-scale motions recovered as special cases.

The Bresse locus was characterized by the vanishing tangential acceleration condition $\ddot{\widehat{\mathbf{Y}}} \cdot \dot{\widehat{\mathbf{Y}}} = 0$. For the selected constant dual-scale motion $\widehat{\rho} = 2 + \varepsilon$, explicit algebraic and parametric representations were obtained, yielding line congruences, ruled-surface families, and degenerate configurations. Computational visualizations were used to illustrate these structures and their dependence on the selected parameters.

From a quantitative viewpoint, an oriented spatial line is represented by six real components $(\mathbf{y}, \mathbf{y}^*)$ subject to two fundamental constraints, leaving four independent degrees of freedom in the line space. The Bresse condition imposes additional algebraic restrictions on this four-dimensional space. In the selected constant-scale example, these restrictions yield lower-dimensional line families parameterized by the free parameters p and q. These results provide a quantitative geometric characterization of the Bresse locus and demonstrate the usefulness of dual-vector calculus for the analysis of equiform spatial motions.

7.1. *Limitations of the study*

The present study has several limitations. The explicit parametric results and visualizations are based on a selected equiform motion and therefore represent a particular case rather than all possible motion configurations. More general parameter choices may also lead to increased symbolic and algebraic complexity. Finally, the present work is theoretical and computational and does not include experimental validation using a specific mechanical or robotic system.

7.2. *Future research directions*

Future research may focus on the following directions:

- **Non-Euclidean extensions:** Extend the present framework to non-Euclidean geometries, including Minkowski and Galilean spaces.
- **Data-driven kinematic analysis:** Develop numerical and data-driven methods for extracting Bresse line structures from experimental motion data.
- **Robotic kinematic applications:** Integrate the dual-space formulation with specific robotic mechanisms to investigate trajectory planning, singular configurations, and related kinematic constraints.

Author contributions

Ali Abdela Ali: Conceptualization, Methodology, Validation, Investigation, Writing–original draft, Supervision; Anas A. M. Arafa: Validation, Supervision; Fahad Abdulaziz Alsidrani: Validation, Writing–review & editing, Visualization, Supervision. All authors have read and approved the final version of the manuscript for publication.

Use of Generative-AI tools declaration

The authors declare that they have not used Artificial Intelligence (AI) tools in the creation of this article.

Acknowledgements

The researchers would like to thank the Deanship of Graduate Studies and Scientific Research at Qassim University (https://www.qu.edu.sa) for financial support (QU-APC-2026).

Conflict of interest

The authors declare that there is no conflict of interest regarding the publication of this article.

References

1. H. W. Guggenheimer, *Differential geometry*, New York: McGraw–Hill, 1963.
2. Ö. Köse, Kinematic differential geometry of a rigid body in spatial motion using dual vector calculus: Part-I, *Appl. Math. Comput.*, **183** (2006), 17–29. https://doi.org/10.1016/j.amc.2006.02.054
3. Ö. Köse, C. C. Sarıoğlu, B. Karabey, İ. Karakılıç, Kinematic differential geometry of a rigid body in spatial motion using dual vector calculus: Part-II, *Appl. Math. Comput.*, **182** (2006), 333–358. https://doi.org/10.1016/j.amc.2006.02.059
4. J. M. McCarthy, G. S. Soh, *Geometric design of linkages*, 2 Eds., New York: Springer, 2011. https://doi.org/10.1007/978-1-4419-7892-9

5. R. A. Hussein, A. A. Ali, Geometry of the line space associated to a given dual ruled surface, *AIMS Math.*, **7** (2022), 8542–8557. https://doi.org/10.3934/math.2022476
6. E. Study, *Geometrie der dynamen: Die zusammensetzung von Kräften und verwandte gegenstände der geometrie*, New York: Cornell University Library, 1903.
7. A. A. Almoneef, R. A. Abdel-Baky, Kinematic differential geometry of a line trajectory in spatial movement, *Axioms*, **12** (2023), 472. https://doi.org/10.3390/axioms12050472
8. F. Mofarreh, R. A. Abdel-Baky, One-parameter hyperbolic dual spherical movements and timelike ruled surfaces, *Symmetry*, **15** (2023), 902. https://doi.org/10.3390/sym15040902
9. Y. L. Li, F. Mofarreh, R. A. Abdel-Baky, Kinematic-geometry of a line trajectory and the invariants of the axodes, *Demonstr. Math.*, **56** (2023), 20220252. https://doi.org/10.1515/dema-2022-0252
10. D. Condurache, A full-body relative orbital motion of spacecraft using dual tensor algebra and dual quaternions, *Mathematics*, **11** (2023), 1366. https://doi.org/10.3390/math11061366
11. X. Wang, H. X. Sun, C. L. Liu, H. W. Song, Dual quaternion operations for rigid body motion and their application to the hand-eye calibration, *Mech. Mach. Theory*, **193** (2024), 105566. https://doi.org/10.1016/j.mechmachtheory.2023.105566
12. J. G. Farias, E. De Pieri, D. Martins, A review on the applications of dual quaternions, *Machines*, **12** (2024), 402. https://doi.org/10.3390/machines12060402
13. A. A. Almoneef, R. A. Abdel-Baky, Timelike line congruences via surface theory in Minkowski 3-space, *AIP Adv.*, **15** (2025), 055125. https://doi.org/10.1063/5.0268437
14. Z. D. Yaqub, H.-P. Schröcker, Rational motions of minimal quaternionic degree with prescribed line trajectories, *Mech. Mach. Theory*, **215** (2025), 106182. https://doi.org/10.1016/j.mechmachtheory.2025.106182
15. C. C. Sarıoğlu, Acceleration and the differential geometry of screws, Master Thesis, Dokuz Eylül University, 2003.
16. V. M. Zatsiorsky, *Kinematics of human motion*, Champaign: Human Kinetics, 1998.